

Molecular MRI Differentiation between Primary Central Nervous System Lymphoma (PCNSL) and High-grade Glioma (HGG) Using Endogenous Protein-based Amide Proton Transfer (APT) Signals

Shanshan Jiang^{1,2}, Hao Yu¹, Xianlong Wang¹, Shilong Lu¹, Yi Zhang², Doon-Hoon Lee², Hye-Young Heo², Jinyuan Zhou², and Zhibo Wen¹

¹Department of Radiology, Zhujiang Hospital of Southern Medical University, Guangzhou, Guangdong, China, ²Department of Radiology, Johns Hopkins University School of Medicine, Baltimore, MD, United States

Target audience: Researchers and clinicians who are interested in clinical CEST imaging applications.

Purpose

PCNSLs present approximately 5% of all primary brain tumors, and the incidence has increased drastically in recent decades¹. PCNSLs are usually treated by chemotherapy and radiotherapy, while HGGs favor a maximal safe resection first. Therefore, the precise preoperative differentiation of PCNSLs and HGGs is of significant practical relevance. APT imaging can generate molecular MRI signals that are based on the amide protons of endogenous mobile proteins and peptides. Previous studies have shown that APT MRI can provide unique information about the grade of malignant HGGs, separate edema from tumor, and differentiate between gliomas and radiation necrosis.²⁻⁵ PCNSLs have not been studied with APT imaging. We aimed to explore the diagnosis performance of APT imaging in the differentiation of PCNSLs and HGGs.

Methods

Thirty-three patients who signed informed consent were recruited, including 11 PCNSL patients and 21 HGG patients. Patients had no clinical history of previous surgery, corticosteroid administration, chemotherapy, or radiotherapy. MRI was done on a Philips 3T MRI scanner (Achieva). The APT imaging parameters were: RF saturation power = 2 μ T; saturation time = 800 ms; slice thickness = 6 mm. To simultaneously acquire APT images and z-spectra, we used a multi-offset, multi-acquisition APT imaging protocol (scan time 3 min). The saturated image at the offset of 15.6 ppm was acquired to calculate the conventional MTR value relating to the semi-solid MT imaging.

The APT-weighted (APTW) image [i.e., $MTR_{asym}(3.5\text{ppm})$] was calculated using the B_0 -corrected data at ± 3.5 ppm. At least five ROIs were drawn on the Gd-enhancing tumor core for each patient. The APTW signal intensity, MTR_{asym} spectrum data, and MTR value were recorded for each ROI. The maximum APTW signal intensity ($APTW_{max}$), the distribution of APTW signal intensities inside the tumor core ($APTW_{max-min}$), as well as the total CEST signal intensity (integral of the whole MTR_{asym} spectrum, $CEST_{total}$) and MTR (corresponding to the ROI with $APTW_{max}$) were reported for each patient. The contralateral normal-appearing white matter (CNAWM) was used for comparison.

Results and Discussion

MTR_{asym} spectrum features: There were increased CEST effects in both tumors (Fig. 1), compared to the CNAWM, particularly at the offsets of 3.5 ppm (APT) and 2.5 ppm (mixed amine CEST). The CEST effects were slightly lower in the lymphoma than in the high-grade glioma.

Image features: For PCNSLs (Fig. 2), T₂W MRI showed a hyperintense lesion (compared to contralateral brain tissue). Gd-T₁W imaging revealed an enhancing tumor core. On the APTW image, most tumor visible on the Gd-T₁W image was homogeneously hyperintense. For HGGs (Fig. 3), the lesion was hyperintense on T₂W image and hypointense in T₁W image, with a heterogeneous Gd-enhancing mass. APTW image clearly identified the tumor core as heterogeneous hyperintense lesion.

Quantitative analysis: APTW signal intensities and distribution inside the tumor core, and total CEST signal intensities were all significantly lower in PCNSLs than in HGGs (Fig. 4). On the contrary, semi-solid-related MTR values were significantly higher in PCNSLs than in HGGs. Relatively higher APTWs (sensitive to mobile cytosolic proteins) and lower MTRs (sensitive to semi-solid chemicals, such as nuclear proteins) were consistent with the histological characteristics of higher nucleus-to-cytoplasm ratios in PCNSLs than in HGGs (Fig. 5).

Conclusion

Our initial data show that APT imaging can differentiate PCNSLs from HGGs. Adding APT to standard MRI sequences would potentially improve the diagnostic accuracy of MRI.

References

- 1) Land et al. CA Cancer J. Clin. 49, 8 (1999).
- 2) Wen et al. NeuroImage 51, 616 (2010).
- 3) Zhou et al. Nature Med. 17, 130 (2011).
- 4) Togao et al. Neuro-oncology 16, 441 (2014).
- 5) Sagiyama et al. PNAS 111, 4542 (2014).

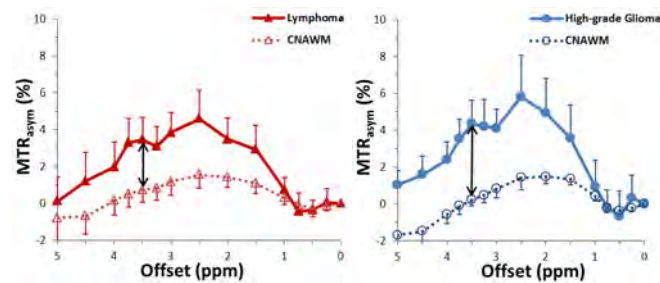


Fig. 1. Average MTR_{asym} spectra of lymphoma and high-grade glioma. The CEST effects were clearly visible in the offset range of 1.5-4 ppm.

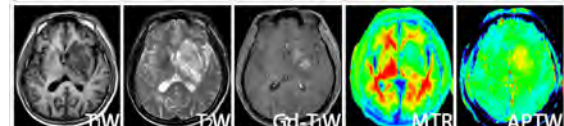


Fig. 2. A 60-year-old man with lymphoma in the left basal ganglion. The Gd-enhancing tumor core had a relatively homogeneous APT signal intensity of 2.44%-3.13%.

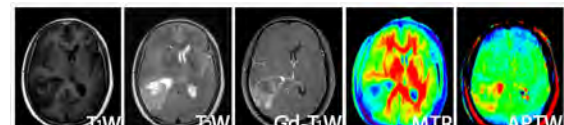


Fig. 3. A 46-year-old man with glioblastoma in the right temporal and occipital lobe. The Gd-enhancing tumor core had a heterogeneous APT signal intensity from 1.59%-3.58%.

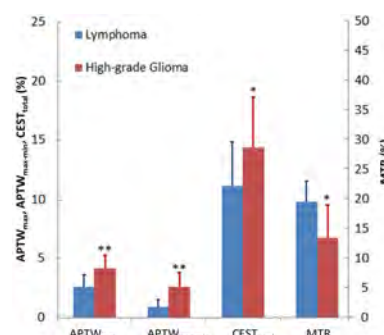


Fig. 4. Comparison of the maximum APTW signal intensities ($APTW_{max}$), the distribution of APTW signal intensities ($APTW_{max-min}$), the total CEST signal intensities ($CEST_{total}$), and the MTR values for high-grade glioma and lymphoma.
*, p < 0.05; **, p < 0.01.

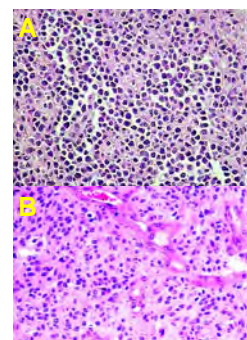


Fig. 5. Optically magnified images (10 \times 20) of H&E-stained sections. (A) A lymphoma showing dense aggregate cells with scanty cytoplasm. The nucleus/cytoplasm ratio was 1.0. (B) A high-grade glioma showing cells with more abundant cytoplasm. The nucleus/cytoplasm ratio was 0.49.